

Stability diagram and growth rate of parametric resonances in Bose-Einstein condensates in one-dimensional optical lattices

C. Tozzo¹, M. Krämer², and F. Dalfovo¹

¹*BEC-INFM and Dipartimento di Fisica,
Università di Trento, I-38050 Povo, Italy*

²*JILA, University of Colorado and
National Institute of Standards and Technology,
Boulder, CO 80309-0440, USA*

(Dated: May 24, 2005)

A Bose-Einstein condensate in an optical lattice exhibits parametric resonances when the intensity of the lattice is periodically modulated in time. These resonances correspond to an exponential growth of the population of counter-propagating Bogoliubov excitations. A suitable linearization of the Gross-Pitaevskii (GP) equation is used to calculate the stability diagram and the growth rates of the unstable modes. The results agree with the ones extracted from time-dependent GP simulations, supporting our previous claim (M. Krämer *et al.*, Phys. Rev. A (2005) in press) concerning the key role of parametric resonances in the response observed by Stöferle *et al.* (Phys. Rev. Lett. **92**, 130403 (2004)) in the superfluid regime. The role of the seed excitations required to trigger the parametric amplification is discussed. The possible amplification of the quantum fluctuations present in the quasiparticle vacuum, beyond GP theory, is also addressed, finding interesting analogies with similar processes in nonlinear quantum optics and with the dynamic Casimir effect. Our results can be used in exploiting parametric instabilities for the purpose of spectroscopy, selective amplification of a particular excitation mode and for establishing a new type of thermometry.

PACS numbers: 03.75.Kk, 03.75.Lm

I. INTRODUCTION

A parametric resonance corresponds to the exponential growth of certain modes of a system induced by the periodic variation of a parameter [1, 2]. It is a very general phenomenon occurring in classical oscillators, in nonlinear optics, in systems governed by Non-Linear Schrödinger equations, and in Hamiltonian chaotic systems. Parametric resonances can also occur in Bose-Einstein condensates made of ultracold atomic gases. From the theoretical side, they have already been investigated in 3D [3, 4, 5] and 2D [6, 7] harmonically trapped condensates, for condensates in oscillating double-well potentials [8, 9, 10] and in deep optical lattices [11]. These investigations are based on suitable effective Hamiltonians in which the interaction between the atoms enters through a mean-field term proportional to the condensate density. Most of them make use of the Gross-Pitaevskii (GP) equation, which has the form of a Non-Linear Schrödinger equation and gives a very accurate description of dilute condensates [12, 13].

In Ref. [14] we have recently shown that parametric resonances can be the origin of the large and broad response observed by Esslinger and co-workers [15, 16, 17] in the superfluid phase of a condensate in an optical lattice. Our claim was based on the results of numerical simulations, namely the integration of the time-dependent GP equation. In the present work we perform a more systematic analysis, by investigating the behavior of Bogoliubov quasiparticles subject to a periodic modulation of the lattice. The purpose is to gain a deeper insight into the process of parametric resonances, in particular

into the conditions for the occurrence of the instability, the growth rates associated with the parametric amplification of an excitation and the role of the initial fluctuations (seed excitations) which trigger the onset of the amplification.

The basic theory is presented in section II. We consider an infinite condensate at zero temperature, subject to a transverse harmonic potential and to a 1D optical lattice along the z -direction, with N atoms per lattice site. The effect of the optical lattice can be expressed through the periodic potential $V(z, t) = s(t)E_R \sin^2(q_B z)$, where $q_B = \pi/d$ is the Bragg wave vector, d is the lattice spacing and s is the lattice depth in units of the recoil energy $E_R = \hbar\omega_R = \hbar^2 q_B^2/2m$. The transverse harmonic confinement, of frequency ω_\perp , is taken to be sufficiently strong to inhibit excitations involving the radial degrees of freedom on the energy scale we are concerned with. Under this assumption, the order parameter can be factorized into a radial Gaussian, having constant width $a_\perp = [\hbar/(m\omega_\perp)]^{1/2}$, times a z and t -dependent order parameter, $\Psi(z, t)$. The latter obeys an effective 1D GP equation which includes the atom-atom interaction through a coupling constant g . We first consider the case of a static optical lattice ($s(t) = s_0$) and we find the Bogoliubov spectrum as a result of the linearization of the GP equation with regard to a small change, $\delta\Psi(z, t)$, of the condensate wave function. Then we study the evolution of the system under a modulation of lattice depth in the form $s(t) = s_0[1 + A \sin(\Omega t)]$. A stability analysis is done in order to find the parametrically unstable modes and calculate their growth rate for given values of the parameters s_0 , A and gn , where $n = N/d$ is the average linear density. We use a Bogoliubov quasiparticle projec-

tion method [21, 22] in order to provide a deeper insight into the mechanisms of instability.

When A is not too large, the main mechanism which drives a parametric resonance is a coupling between pairs of counter-propagating Bogoliubov axial excitations of frequencies ω_{jk} and $\omega_{j'k}$, where k is the wave vector and j and j' are Bloch band indexes. The multi-mode stability analysis then reduces to a two-mode approximation. The resonance condition becomes $\Omega = \omega_{jk} + \omega_{j'k}$, which yields $\Omega = 2\omega_{0k}$ for axial phonons in the lowest Bloch band. This approximation is discussed in section III, where we show that the parameters s_0 , A and gn can be combined in a single parameter $\bar{\gamma} = (1/2)s_0A\Omega\Gamma_{+-}^{jj'}$, which contains all relevant information about the stability diagram and the growth rate. The quantity $\Gamma_{+-}^{jj'}$ depends on s_0 and k and can be calculated by solving the Bogoliubov equations for different lattice depths. It describes the coupling between Bogoliubov modes belonging to the j and j' bands and having opposite quasi-momenta. This coupling is mediated by the time-dependence of the lattice potential. In the tight binding regime, i.e. when the lattice depth is large enough to split up the condensate in almost independent condensates at each lattice site, a semi-analytic result can be derived for the quantity $\bar{\gamma}$ describing the parametric resonance of modes of the lowest Bogoliubov band. In this case, in fact, the quantity Γ_{+-}^{00} can be simply expressed through the s -dependence of the effective mass and the compressibility of the condensate. This regime is discussed in section IV.

The numerical results of the stability analysis are shown in section V together with those of the two-mode and tight-binding approximations. The two-mode approximation turns out to be very accurate in the whole range of parameters here considered. At large s_0 the tight binding expressions work well. The approach to this regime is faster when the mean-field interaction is small (i.e., small values of gn).

In section VI the results obtained in the previous sections by linearizing the GP equation for an infinite condensate are compared with those obtained from the numerical integration of the time dependent GP equation. We perform GP simulations for an infinite condensate, as well as a trapped condensate similar to the ones of the experiments of Refs. [15, 16, 17] and of our previous calculations of Ref. [14]. The agreement is good. This confirms the overall picture for the key role played by the parametric instability of Bogoliubov excitations in the observed large and broad response of the condensate to the modulation of the lattice depth. These results also support the possibility to use parametric resonances as a tool for spectroscopic studies of Bogoliubov excitations, for a selective amplification of certain modes and for the characterization of thermal and/or quantum fluctuations in trapped condensates. A brief discussion on how parametric resonances can give information about thermal and quantum fluctuations is given in section VII.

II. BOGOLIUBOV EXCITATIONS IN AN AMPLITUDE MODULATED LATTICE

A. Bogoliubov spectrum in a static lattice

Let us consider a dilute condensate made of atoms with mass m and s -wave scattering length a , whose order parameter obeys the time-dependent GP equation [12, 13]

$$i\hbar\partial_t\Psi = \left[-\frac{\hbar^2}{2m}\nabla^2 + V + g_{3D}N|\Psi|^2 \right] \Psi, \quad (1)$$

where Ψ is normalized to 1, N is the number of particles and $g_{3D} = 4\pi\hbar^2a/m$. The potential V is the sum of the harmonic trap and the optical lattice. The 1D optical lattice is taken to be oriented along the z -direction with lattice depth s , spacing d , Bragg wave vector $q_B = \pi/d$ and recoil energy $E_R = \hbar\omega_R = \hbar^2q_B^2/2m$. The transverse harmonic confinement is assumed to be sufficiently strong to freeze the radial degrees of freedom, so that the order parameter is simply a Gaussian in the transverse direction, having constant width $a_\perp = [\hbar/(m\omega_\perp)]^{1/2}$. Under this condition, the 3D GP equation (1) reduces to an effective 1D GP equation for a purely axial order parameter $\Psi(z, t)$:

$$i\hbar\partial_t\Psi = \left[-\frac{\hbar^2}{2m}\partial_z^2 + sE_R\sin^2(q_Bz) + gnd|\Psi|^2 \right] \Psi. \quad (2)$$

Here the normalization condition is $\int_{-d/2}^{d/2} dz|\Psi|^2 = 1$, while $nd = N$ is the number of atoms per lattice site and n is the average linear density. The quantity $g = g_{3D}/2\pi a_\perp^2$ is an effective 1D coupling constant accounting for the atom-atom interaction. With this choice, Eq. (2) also coincides with that of Ref. [18] for a uniform condensate in a 1D lattice.

When the condensate is weakly perturbed, the order parameter can be written as

$$\Psi(z, t) = e^{-i\mu t/\hbar}[\Psi_0(z) + \delta\Psi(z, t)] \quad (3)$$

where Ψ_0 is the groundstate solution of the stationary GP equation

$$\left[-\frac{\hbar^2}{2m}\partial_z^2 + sE_R\sin^2(q_Bz) + gnd|\Psi_0|^2 \right] \Psi_0 = \mu\Psi_0 \quad (4)$$

and μ is the corresponding chemical potential. The small variation $\delta\Psi$ can be expressed in terms of Bogoliubov excitations,

$$\delta\Psi = \sum_{jk} c_{jk}u_{jk}(z)e^{-i\omega_{jk}t} + c_{jk}^*v_{jk}^*(z)e^{i\omega_{jk}t}, \quad (5)$$

where c_{jk} are complex coefficients. Due to the periodicity of the external potential, the Bogoliubov quasiparticle amplitudes u_{jk} and v_{jk} have the form of Bloch functions $u_{jk} = \exp(ikz)\tilde{u}_{jk}$ and $v_{jk} = \exp(ikz)\tilde{v}_{jk}$, where \tilde{u}_{jk}

and \tilde{v}_{jk} are periodic with period d . The excitations are labelled by their quasimomentum $\hbar k$ and the Bloch band index j .

By inserting (5) into (2) and linearizing with respect to $\delta\Psi$ one finds that the amplitudes u_{jk} and v_{jk} are solutions of the eigenvalue problem

$$\mathcal{L}(s, k) \begin{pmatrix} \tilde{u}_{jk} \\ \tilde{v}_{jk} \end{pmatrix} = \hbar\omega_{jk} \begin{pmatrix} \tilde{u}_{jk} \\ \tilde{v}_{jk} \end{pmatrix} \quad (6)$$

where the matrix $\mathcal{L}(s, k)$ is given by

$$\mathcal{L}(s, k) = \begin{pmatrix} H(s, k) & gnd\Psi_0^2 \\ -gnd\Psi_0^{*2} & -H(s, k) \end{pmatrix} \quad (7)$$

and we have defined

$$\begin{aligned} H(s, k) = & -\frac{\hbar^2}{2m}(\partial_z + ik)^2 + sE_R \sin^2(q_B z) \\ & + 2gnd |\Psi_0|^2 - \mu. \end{aligned} \quad (8)$$

Moreover, for any given k the solutions \tilde{u}_{jk} and \tilde{v}_{jk} obey the ortho-normalization conditions

$$\int_{-d/2}^{d/2} dz (\tilde{u}_{jk}^* \tilde{u}_{j'k} - \tilde{v}_{jk}^* \tilde{v}_{j'k}) = \delta_{jj'}, \quad (9)$$

$$\int_{-d/2}^{d/2} dz (\tilde{u}_{jk} \tilde{v}_{j',-k} - \tilde{u}_{j',-k} \tilde{v}_{jk}) = 0. \quad (10)$$

Equations (6) can be solved numerically to get the amplitudes \tilde{u}_{jk} , \tilde{v}_{jk} and the Bogoliubov band spectrum $\hbar\omega_{jk}$ for given values of the lattice depth $s = s_0$ and interaction parameter gn . In Fig. 1 we plot the lowest three bands as obtained for $s_0 = 4$ and $gn = 0.72E_R$. The latter value is chosen as the axial average of the interaction parameter in the experimental setting of [15]. The lowest band exhibits a linear dispersion for $k \rightarrow 0$ as expected for long wavelength Bogoliubov phonons traveling along z at the speed of sound. This type of spectra have been already discussed in the recent literature [18, 19, 20]. Here we use the results of Fig. 1 as a basis for the subsequent discussion of parametric resonances.

B. Modulation of the lattice depth

Let us consider a periodic modulation of the lattice depth in the form

$$s(t) = s_0[1 + A \sin(\Omega t)], \quad (11)$$

with $A \ll 1$. The dynamics induced by this modulation can still be described by Eqs. (2) and (3). To this purpose we assume that Ψ_0 is, at any time t , the stationary solution of (4) for $s = s(t)$. Both Ψ_0 and μ are now functions of t via their dependence on $s(t)$. Then we insert again (3) into (2), take s as in (11), and look for an equation

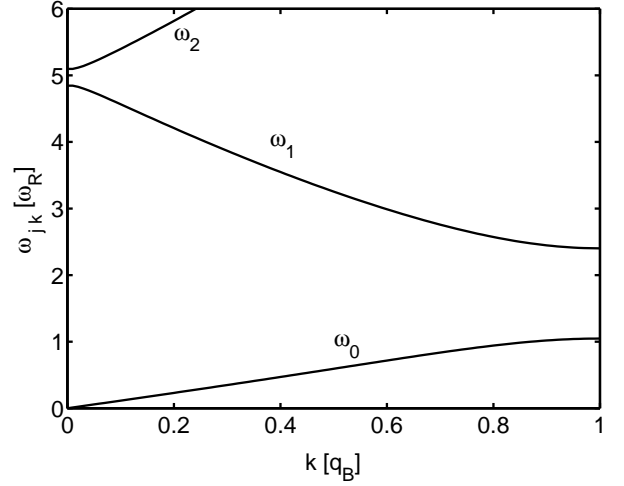


FIG. 1: Lowest bands in the Bogoliubov spectrum of a cylindrical condensate in a periodic lattice, obeying Eq. (2) with $s = s_0 = 4$ and $gn = 0.72E_R$. The range of k corresponds to half of the first Brillouin zone. We use the shorthand notation ω_0 , ω_1 and ω_2 to indicate the Bogoliubov bands whose dispersion relation is ω_{0k} , ω_{1k} and ω_{2k} .

of motion for the small part $\delta\Psi$. Up to linear terms in $\delta\Psi$, one gets

$$\begin{aligned} i\partial_t \delta\Psi = & [H(s, k) + 2gnd |\Psi_0|^2 - \mu] \delta\Psi \\ & + gnd\Psi_0^2 \delta\Psi^* + \dot{s} [i\partial_s + (\partial_s \mu)t/\hbar] \Psi_0. \end{aligned} \quad (12)$$

The inhomogeneous term, proportional to \dot{s} , behaves like a source of excitations in the linear response regime. It creates excitations out of the condensate when Ω is resonant with a Bogoliubov frequency ω_{jk} at $k = 0$. For symmetry reasons, the first resonance occurs at the bottom of the ω_2 band. In the case of Fig. 1 this amounts to $\Omega = \omega_2(k = 0) \simeq 5.1E_R/\hbar$. Similar resonances can be found at larger frequencies. If A is small and the modulation time is long, this type of excitation processes only occurs in narrow and well separated intervals of Ω . Except in these intervals, the inhomogeneous term in Eq. (12) can be safely ignored. In the range of Ω of the two lowest Bogoliubov bands ω_0 and ω_1 , for instance, this approximation is expected to work well, as confirmed also by the comparison with GP simulations (see section VI below). In the same range, also the assumption that Ψ_0 adiabatically follows the lattice modulation is expected to be valid. Finally, the periodicity of the system allows one to write the unknown function $\delta\Psi(z, t)$ in the form of a Bloch wave expansion

$$\delta\Psi(z, t) = \sum_{k>0} \tilde{a}_{+k}(z, t) e^{ikz} + \tilde{a}_{-k}^*(z, t) e^{-ikz}, \quad (13)$$

where the coefficients $\tilde{a}_k(z, t)$ are periodic in z with period d . Neglecting the last term in (12) and inserting the

ansatz (13), one finally gets

$$i\hbar\partial_t \begin{pmatrix} \tilde{a}_{+k} \\ \tilde{a}_{-k} \end{pmatrix} = \mathcal{L}(s, k) \begin{pmatrix} \tilde{a}_{+k} \\ \tilde{a}_{-k} \end{pmatrix}. \quad (14)$$

This is the equation of motion for $\delta\Psi$. It contains the external parameter $s(t)$, which varies periodically in time, and hence it can exhibit parametric instabilities. We perform the stability analysis of this equation using the method explained in section II C below.

In order to give a more transparent view of the processes involved in Eq. (14), one can use a suitable basis of Bogoliubov states [21, 22]. Let us write

$$\begin{pmatrix} \tilde{a}_{+k} \\ \tilde{a}_{-k} \end{pmatrix} = \sum_j \left[c_{jk} \begin{pmatrix} \tilde{u}_{jk} \\ \tilde{v}_{jk} \end{pmatrix} + c_{j,-k}^* \begin{pmatrix} \tilde{v}_{j,-k}^* \\ \tilde{u}_{j,-k}^* \end{pmatrix} \right] \quad (15)$$

where \tilde{u}_{jk} , \tilde{v}_{jk} denote the solutions of (6) at the lattice depth $s(t)$. This corresponds to the projection of $\delta\Psi$, at time t , onto the instantaneous Bogoliubov modes at lattice depth $s(t)$. Inserting (15) into (14) and using (9)-(10), one finds the following equations for the time-dependent coefficients c_{jk} :

$$i\partial_t c_{jk} = \omega_{jk} c_{jk} - i\dot{s} \sum_{j'} \left[\Gamma_{++}^{jj'} c_{j'k} + \Gamma_{+-}^{jj'} c_{j',-k}^* \right] \quad (16)$$

$$i\partial_t c_{j,-k}^* = -\omega_{jk} c_{j,-k}^* - i\dot{s} \sum_{j'} \left[\Gamma_{+-}^{jj'} c_{j'k} + \Gamma_{++}^{jj'} c_{j',-k}^* \right], \quad (17)$$

where

$$\Gamma_{++}^{jj'} = \int_{-d/2}^{d/2} dz (\tilde{u}_{jk}^* \partial_s \tilde{u}_{j'k} - \tilde{v}_{jk}^* \partial_s \tilde{v}_{j'k}), \quad (18)$$

$$\Gamma_{+-}^{jj'}(s) = \int_{-d/2}^{d/2} dz (\tilde{u}_{jk}^* \partial_s \tilde{v}_{j',-k}^* - \tilde{v}_{jk}^* \partial_s \tilde{u}_{j',-k}^*). \quad (19)$$

In deriving (16)-(17) we have used the relations $\tilde{u}_{jk} = \tilde{u}_{j,-k}^*$ and $\tilde{v}_{jk} = \tilde{v}_{j,-k}^*$, which follows from the fact that the groundstate wavefunction can be chosen real (zero current).

Eqs. (16)-(17) reveal that the time-dependence of the lattice depth ($\dot{s} \neq 0$) brings about a coupling between Bogoliubov excitations with the same $|k|$. In particular, the quantity $\Gamma_{++}^{jj'}$ accounts for the scattering of excitations from the perturbation, that is a process in which an excitation in the band j is scattered into the band j' without changing its quasimomentum k . This happens resonantly when Ω is equal to the frequency difference between two bands at the same k . One can easily prove that this process does not vary the total number of excitations [23]. Conversely, the quantity $\Gamma_{+-}^{jj'}$ describes the coupling between counter-propagating excitations. As we will show in the following, this quantity causes an exponential growth of the number of excitations and is thus responsible for the parametric instability. It is worth noticing that $\Gamma_{+-}^{jj'} = 0$ if $gn = 0$ and hence a noninteracting gas, obeying the Schrödinger equation, does not exhibit parametric resonances.

C. Stability analysis

In order to find the parametrically unstable solutions of the linear equation (14) we follow the procedure discussed in Ref. [24]. The dynamics is determined by the operator \mathcal{L} , which changes in time *via* its dependence on $s(t)$. The lattice modulation is periodic with period $T = 2\pi/\Omega$. Therefore the operator \mathcal{L} has the same periodicity and can be expressed by means of the Fourier representation

$$\mathcal{L}(t) = \sum_{\nu=-\infty}^{+\infty} \mathcal{L}^{(\nu)} e^{i\nu \Omega t}, \quad (20)$$

where ν is integer and the operators $\mathcal{L}^{(\nu)}$ do not depend on time. Thanks to Floquet theorem [25], any solution of (14) can be written in the form

$$\begin{pmatrix} \tilde{a}_{+k}(t) \\ \tilde{a}_{-k}(t) \end{pmatrix} = e^{\lambda t} \begin{pmatrix} \tilde{a}'_{+k}(t) \\ \tilde{a}'_{-k}(t) \end{pmatrix}, \quad (21)$$

where λ is a complex constant and the functions $\tilde{a}'_{\pm k}(t)$ are periodic of period T . This periodicity allows one to expand $\tilde{a}'_{\pm k}$ in the Fourier series

$$\tilde{a}'_{\pm k}(t) = \sum_{\nu=-\infty}^{+\infty} \tilde{a}_{\pm k}^{(\nu)} e^{i\nu \Omega t}. \quad (22)$$

Finally, by using Eqs. (20)-(22) one can rewrite Eq. (14) in the form

$$i\lambda \begin{pmatrix} \tilde{a}_{+k}^{(\nu)} \\ \tilde{a}_{-k}^{(\nu)} \end{pmatrix} = \nu \hbar \Omega \begin{pmatrix} \tilde{a}_{+k}^{(\nu)} \\ \tilde{a}_{-k}^{(\nu)} \end{pmatrix} + \sum_{\mu=-\infty}^{+\infty} \mathcal{L}^{(\mu-\nu)} \begin{pmatrix} \tilde{a}_{+k}^{(\mu)} \\ \tilde{a}_{-k}^{(\mu)} \end{pmatrix}. \quad (23)$$

From the solutions of this eigenvalue problem one obtains the complex eigenvalues λ as a function of k and Ω . In practice, the solution can be found by truncating the series (22) at a certain ν so that the problem is reduced to a matrix diagonalization. In our case, we obtain a very good convergence by cutting at ν of the order of 10.

We then define the growth rate γ of a Bogoliubov mode as the real part of λ :

$$\gamma = \text{Re}(\lambda). \quad (24)$$

This quantity fixes the character of the corresponding eigenfunction. If $\gamma \leq 0$ then $|\tilde{a}_{\pm k}(t)|$ is always bound and we say that the mode $\pm k$ is parametrically stable. On the contrary, if $\gamma > 0$ the corresponding eigenfunction describes an unstable mode whose population exponentially increases in time. For a given modulation frequency Ω we say that the condensate is parametrically stable if all eigenfunctions of (23) are stable. By using symmetry properties analogous to the ortho-normality relations (9) and (10), one can prove that the condensate is parametrically stable if and only if $\gamma = 0$ for all modes. The results of this stability analysis will be given in section V.

III. TWO-MODE APPROXIMATION

According to Eqs. (16)-(17), the evolution of a certain mode is, in principle, coupled to the modes of all bands with the same $|k|$. However, one might expect that each resonance essentially arises from the coupling of a pair of counter-propagating modes, the influence of all the others being negligible. In our formalism, this is equivalent to replacing the sum over j' in Eqs. (16)-(17) with a single term. The problem is thus reduced to the solution of the coupled equations

$$i\partial_t \begin{pmatrix} c_{jk} \\ c_{j',-k}^* \end{pmatrix} = \begin{pmatrix} \omega_{jk} - i\dot{s}\Gamma_{++}^{jj'} & -i\dot{s}\Gamma_{+-}^{jj'} \\ -i\dot{s}\Gamma_{+-}^{jj'} & -\omega_{j'k} - i\dot{s}\Gamma_{++}^{jj'} \end{pmatrix} \begin{pmatrix} c_{jk} \\ c_{j',-k}^* \end{pmatrix} \quad (25)$$

for the coefficients c_{jk} and $c_{j',-k}$ of the $\pm k$ -modes in the band j and j' respectively. The coupling $\Gamma_{+-}^{jj'}$ is the same already given in (19).

The modulation (11) of the lattice explicitly enters the two-mode equation (25) through the term $\dot{s} = As_0\Omega \cos(\Omega t)$ in the matrix elements. An additional implicit dependence arises from the s -dependence of $\omega_{jk}, \omega_{j'k}, \Gamma_{++}^{jj'}$ and $\Gamma_{+-}^{jj'}$. In order to investigate the regime of small modulation amplitude, one can linearize Eq. (25) with respect to A , keeping only the leading order of each matrix element. One obtains

$$i\partial_t \begin{pmatrix} c_{jk} \\ c_{j',-k}^* \end{pmatrix} = \begin{pmatrix} \omega_{jk} & -i2\bar{\gamma} \cos(\Omega t) \\ -i2\bar{\gamma} \cos(\Omega t) & -\omega_{j'k} \end{pmatrix} \begin{pmatrix} c_{jk} \\ c_{j',-k}^* \end{pmatrix} \quad (26)$$

where

$$\bar{\gamma} = \frac{1}{2}As_0\Omega(\Gamma_{+-}^{jj'})_{s=s_0} \quad (27)$$

and

$$\omega_{jk} = (\omega_{jk})_{s=s_0}. \quad (28)$$

A further simplification is obtained by neglecting the coupling between resonances at $\pm\Omega$, which is justified when the modulation time is much longer than Ω^{-1} . This allows one to replace $2\cos(\Omega t)$ with $\exp(i\Omega t)$, so that Eq. (26) yields the two coupled equations

$$\partial_t f_{jk} = -\bar{\gamma}e^{i(\omega_{j'k} + \omega_{jk} - \Omega)t} f_{j',-k}^* \quad (29)$$

$$\partial_t f_{j',-k} = -\bar{\gamma}e^{i(\omega_{j'k} + \omega_{jk} - \Omega)t} f_{jk}^* \quad (30)$$

where we have introduced the new variable $f_{jk} = e^{i\omega_{jk}t}c_{jk}$. By inserting (30) in the time derivative of (29), one gets

$$[\partial_t^2 - i(\omega_{jk} + \omega_{j'k} - \Omega)\partial_t - |\bar{\gamma}|^2] f_{jk}(t) = 0 \quad (31)$$

with initial conditions

$$f_{jk}(0) = c_{jk}(0) \quad ; \quad (\partial_t f_{jk})_{t=0} = -\bar{\gamma}c_{j',-k}^*(0). \quad (32)$$

One can easily see that the solutions of Eq. (31) exhibit an exponential growth within the unstable region $|\omega_{jk} + \omega_{j'k} - \Omega| < 2|\bar{\gamma}|$, where the growth rate is found to be

$$\gamma = \frac{1}{2}[4|\bar{\gamma}|^2 - (\omega_{jk} + \omega_{j'k} - \Omega)^2]^{1/2}. \quad (33)$$

This also implies that the maximal growth occurs at the rate

$$\gamma_{\max} = |\bar{\gamma}| \quad (34)$$

when the resonance condition

$$\Omega = \omega_{jk} + \omega_{j'k} \quad (35)$$

is met. The width of the unstable region is $2|\bar{\gamma}|$. By recalling definition (27), one sees that both the maximum rate and the width of the unstable region are proportional to the modulation amplitude A . We notice that, when the coupling occurs between counter-propagating modes in the same Bloch band ($j = j'$), the resonance condition is simply $\Omega = 2\omega_{jk}$. In this case, by using the properties (9)-(10), it is also possible to show that $\text{Im}[\Gamma_{+-}^{jj}] = 0$ and $\Gamma_{++}^{jj} = 0$.

These are the main results of the two-mode approximation. We note that the evaluation of the growth rate (33) only requires the solution of the Bogoliubov equations (6) at s_0 yielding the frequencies $\omega_{jk}, \omega_{j'k}$ and the coupling element $\Gamma_{+-}^{jj'}$.

A further advantage of the two-mode approximation is that it allows one to characterize the role of the seed excitations. Let us concentrate for simplicity on the case of modes satisfying the resonant condition $\Omega = \omega_{jk} + \omega_{j'k}$. The solution of Eq. (31) with initial conditions (32) has the form

$$f_{jk}(t) = \eta e^{\gamma_{\max}t} + \eta' e^{-\gamma_{\max}t}, \quad (36)$$

where

$$\eta = \frac{1}{2}[c_{jk}(0) - c_{j',-k}^*(0)e^{i\phi}] \quad (37)$$

$$\eta' = \frac{1}{2}[c_{jk}(0) + c_{j',-k}^*(0)e^{i\phi}] \quad (38)$$

and $\phi = \text{phase}(\bar{\gamma})$. For long time ($t \gg \gamma_{\max}^{-1}$), the second term in (36) vanishes and the population of both resonant modes have the same exponential growth with rate γ_{\max} . The coefficient η is related to the initial population of the Bogoliubov modes (seed excitations) through Eq. (37). More precisely, the parametric resonance amplifies a quadrature of Bogoliubov excitations which is phase locked with the perturbation [26, 27], and η plays the role of an effective seed. It is worth stressing that exponential growth, i.e., the parametric instability, only occurs if the Bogoliubov modes are already populated at the initial time ($\eta \neq 0$). In section VII we will discuss how this can be related to thermal and/or quantum fluctuations.

IV. TIGHT BINDING REGIME

As the lattice is made deeper one enters the tight binding regime where the condensate atoms are strongly localized near the minima of the lattice potential and only next neighbor Wannier functions have nonvanishing overlap. In this regime, one can derive an analytic expression for the lowest Bogoliubov band (see for example [18])

$$\hbar\omega_0 = \sqrt{\varepsilon_0(\varepsilon_0 + 2\kappa^{-1})}, \quad (39)$$

with $\varepsilon_0 = 2\delta \sin(kd/2)^2$. The tunnelling parameter δ is related to the effective mass through the relation $\delta = (2/\pi^2)(m/m^*)E_R$, while $\kappa^{-1} = n\partial\mu/\partial n$ is the inverse of the compressibility. Furthermore, as discussed in [18], the Bogoliubov amplitudes of the lowest band become proportional to stationary Bloch state solutions φ_k of the GP equation, $u_{0k} = U_k\varphi_k$, $v_{0k} = V_k\varphi_k$ with

$$U_k = \frac{\varepsilon_0 + \hbar\omega_0}{2\sqrt{\hbar\omega_0\varepsilon_0}}, \quad (40)$$

$$V_k = \frac{\varepsilon_0 - \hbar\omega_0}{2\sqrt{\hbar\omega_0\varepsilon_0}}. \quad (41)$$

One can use these results to calculate the coupling element Γ_{+-}^{00} in Eq.(19). The result is

$$\Gamma_{+-}^{00} = U_k\partial_s V_k - V_k\partial_s U_k. \quad (42)$$

Inserting Eqs. (40)-(41), one obtains

$$\begin{aligned} \Gamma_{+-}^{00} &= \frac{\omega_0\partial_s\varepsilon_0 - \varepsilon_0\partial_s\omega_0}{2\varepsilon\omega} \\ &= \frac{\kappa^{-1}\partial_s\delta - \delta\partial_s\kappa^{-1}}{2\delta(\varepsilon_0 + 2\kappa^{-1})}. \end{aligned} \quad (43)$$

In the tight binding regime the coupling Γ_{+-}^{00} is hence directly related to the lattice depth dependence of compressibility and tunnelling (effective mass). Expression (43) allows for a comparison with the two mode approximation, as we will see in the next section.

A nice result is obtained by inserting expression (43) into Eq. (27), using the definition (34) and taking the $s_0 \gg 1$ limit. One finds

$$\gamma_{\max} = \frac{As_0\Omega}{4c_{\text{hd}}} \left. \frac{\partial c_{\text{hd}}}{\partial s} \right|_{s=s_0}, \quad (44)$$

with

$$c_{\text{hd}} = (m^*\kappa)^{-1/2}. \quad (45)$$

The latter coincides with the Bogoliubov sound velocity of the hydrodynamic approach of Ref. [18]. Therefore, in the limit of very large s_0 , where the order parameter Ψ_0 can be assumed to be time-independent and the fluctuating part $\delta\Psi$ can be described in terms of hydrodynamic phonons with linear dispersion $\omega_{0k} = c_{\text{hd}}k$, the growth rate of the parametric resonance turns out to be determined by the change in sound velocity induced by the lattice modulation.

V. RESULTS

In this section, we present the results of the stability analysis of section II together with the ones of the two-mode and tight-binding approximations of sections III and IV.

Let us first discuss the limit of a small modulation amplitude, $A \rightarrow 0$. In this limit the results of the stability analysis of Eq. (14) are found to exactly coincide with the ones of the two-mode approximation. The parametrically unstable regions in the (Ω, k) plane have a vanishingly small width, falling onto the lines where the resonance condition (35) is fulfilled. The lowest lines are plotted in Fig. 2. The different line styles indicate different pairs of resonant modes. By direct comparison with the spectrum in Fig. 1, one sees that the first resonance is encountered at twice the frequency of the lowest Bogoliubov band, $\Omega = 2\omega_0$ (solid line). The next resonance is found when Ω is the sum of the frequencies of the lowest and the next Bogoliubov band, $\Omega = \omega_0 + \omega_1$ (dashed line). Further resonances occur at twice the frequencies of the first excited band, $\Omega = 2\omega_1$ (dash-dotted line), at the sum of frequencies of the lowest and the second excited bands, $\Omega = \omega_0 + \omega_2$ (dotted line), and so on. One or more parametric excitations occur for any value of Ω , except within the gap between $2\omega_0$ and $(\omega_0 + \omega_1)$ resonances at zone boundary.

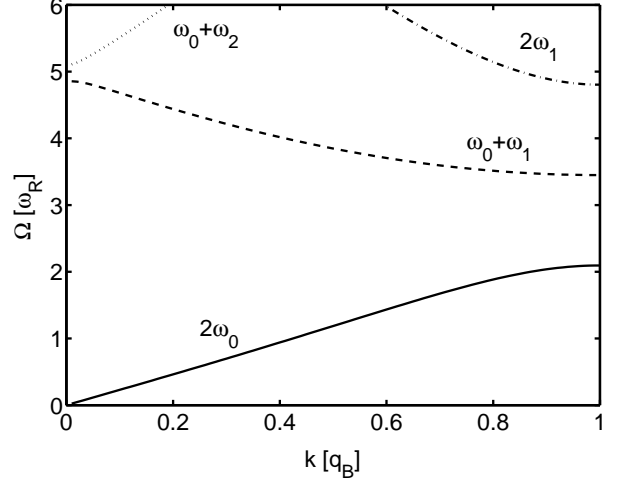


FIG. 2: Position of parametric resonances for $s_0 = 4$, $gn = 0.72E_R$ and for a small modulation amplitude, $A \rightarrow 0$. See Fig.1 for the Bogoliubov spectrum ω_{jk} with the same parameters.

For small A , both the growth rate of the unstable modes and the width of the instability regions are found to be proportional to A . In Fig. 3 we plot the growth rate on resonance, $\gamma = \gamma_{\max}$, divided by A , for the same resonances of Fig. 2. Solid lines are the numerical results of the stability analysis of section II C (see definition (24)) for $A < 0.01$, while empty circles represent the results of the two-mode approximation (see Eqs. (27)

and (34)). The very good agreement between the exact multi-mode calculations and the two-mode results shows that, for small A , the essential mechanism underlying the parametric process is fully captured by the two-mode approximation. In Fig. 3 the quantity γ/A takes values ranging from 0 to typically $\sim 0.2\omega_R$, which implies that, on resonance, parametric amplification occurs on a time scale much longer than ω_R^{-1} .

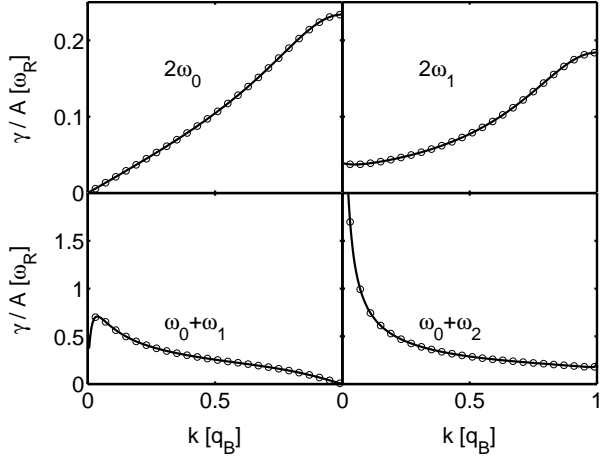


FIG. 3: Growth rates of parametric amplification for $s_0 = 4$, $gn = 0.72E_R$ in the small A limit. The resonances are the same as in Fig. 2. Lines: results of the stability analysis of Eq. (14). Different values of A in the range $A < 0.01$ give the same curves for γ/A . Circles: Eqs. (27) and (34) of the two-mode approximation, with $\Gamma_{+-}^{jj'}$ given in (19) and calculated by solving the Bogoliubov equations (6) at $s_0 = 4$.

Within the two-mode approximation, two excitations of frequency ω_{ik} and ω_{jk} are unstable when $|\omega_{ik} + \omega_{jk} - \Omega| < 2|\bar{\gamma}|$, where $|\bar{\gamma}| = \gamma_{\max}$ is the maximal growth rate on resonance. The values of the maximal growth rate plotted in Fig. 3 thus indicate that, at small values of A , one is generally dealing with very narrow resonances. For the parameters used in Figs. 2 and 3 ($s_0 = 4$ and $gn = 0.72E_R$) and for $A < 0.01$, the width is less than 1% of the resonance frequency.

The overall qualitative picture is preserved when the modulation amplitude A is tuned to experimentally relevant values. An example is given in Fig. 4 where we plot the stability diagram in the energy range of the $2\omega_0$ -resonance obtained with the stability analysis of section II C for $A = 0.1$. The main branch remains centered around the resonance condition $\Omega = 2\omega_{0k}$. The shape of $\gamma(k, \Omega)$ near resonance is very well approximated by Eq. (33), which yields $\gamma = [\gamma_{\max}^2 - (\omega_{0k} - \Omega/2)^2]^{1/2}$. The maximal growth rate γ_{\max} is plotted as a dot-dashed line in Fig. 5. Figure 4 shows that the $2\omega_0$ -resonance remains narrow even for relatively large A , the finite width becoming noticeable only close to the band edge where it reaches about 5% of the resonance frequency. However, new features appear, which are due to very weak resonances of higher order in A . In particular, one clearly sees

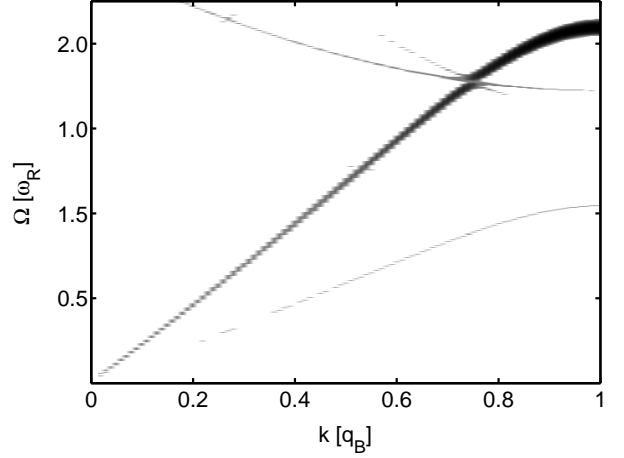


FIG. 4: Stability diagram in the (k, Ω) -plane obtained with the procedure of section II C for $A = 0.1$, $s_0 = 4$ and $gn = 0.72E_R$. The lightest level of grey in the grey-scale represents all modes having $10^{-10} < \gamma < 10^{-3}$. The main branch corresponds to the $2\omega_0$ -resonance, whose maximal growth rate γ_{\max} grows with k as shown in Fig. 5. The other weak branches are higher order parametric resonances.

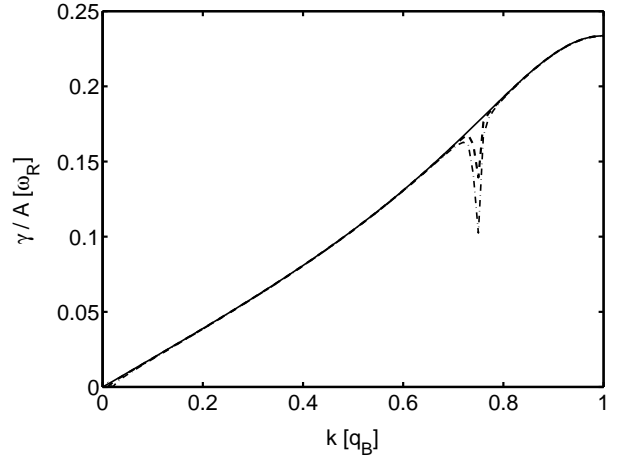


FIG. 5: Growth rate γ/A for the $2\omega_0$ -resonance ($\Omega = 2\omega_{0k}$) obtained with the stability analysis of Eq. (14) with $s_0 = 4$, $gn = 0.72E_R$ and $A < 0.01$ (solid line) and $A = 0.05$ (dashed) and $A = 0.1$ (dot-dashed).

narrow unstable regions at frequency ω_0 and $(\omega_0 + \omega_1)/2$. The growth rate and the width of these resonances are both of order A^2 , so that they are not accounted for by the two-mode approximation of section III. The resonances at $(\omega_0 + \omega_1)/2$ and $2\omega_0$ exhibit a crossing, giving rise to a complex structure in the stability diagram. For our values of s_0 and gn , the crossing occurs at about $k = 0.75q_B$. The effects of this crossing are also visible in the growth rate of the $2\omega_0$ resonance. In Fig. 5 we plot γ/A calculated at $\Omega = 2\omega_{0k}$ for different values of

A. The solid line is the same as in the top-left panel of Fig. 3 and corresponds to $A < 0.01$. The dashed and dot-dashed lines correspond to $A = 0.05$ and 0.1 , respectively. The figure confirms that γ remains directly proportional to A up to relatively large values of A , except in a narrow region near $k \sim 0.75q_B$, in correspondence with the crossing point.

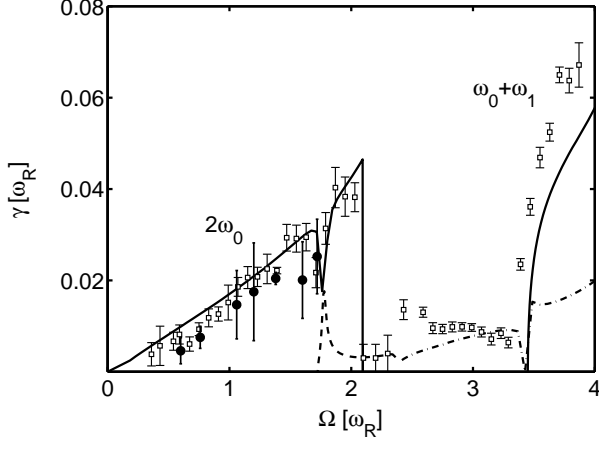


FIG. 6: Growth rate γ as a function of the modulation frequency Ω . The lines are the results of the stability analysis of section II for $A = 0.2$, $s_0 = 4$ and $gn = 0.72E_R$. In particular, the two solid lines are the resonances of order A at $2\omega_0$ and $\omega_0 + \omega_1$, while the dashed and dot-dashed lines are the weaker resonances of order A^2 at $(\omega_0 + \omega_1)/2$ and $(\omega_0 + \omega_2)/2$, respectively. Empty circles are extracted from the time evolution of the incoherent fraction $\delta N/N$ in GP simulations on a cylindrical condensate, unbound along z and harmonically confined in the transverse direction. Solid circles come from GP simulations as well, but for a condensate which is harmonically confined also along z , similar to the trapped condensates of the experiments of Ref. [15, 16, 17].

The growth rate can also be plotted as a function of the modulation frequency Ω , as done in Fig. 6 where we show the results for $A = 0.2$. The solid lines represent the growth rate of the two resonances, of order A , at $2\omega_0$ and $\omega_0 + \omega_1$, while the dashed and dot-dashed lines correspond to the weaker resonances, of order A^2 , at $(\omega_0 + \omega_1)/2$ and $(\omega_0 + \omega_2)/2$, respectively. The growth rate of the ω_0 resonance is very small on this scale and it is not shown. The points with error bars come from GP simulations and will be discussed in the next section.

Coming back to the $A \rightarrow 0$ limit, we notice that, as shown in Fig. 3, the growth rates of the various types of resonances significantly differ in their dependence on the quasimomentum k . Apart from a slight upward bend at around half the Brillouin zone, the curve for the $2\omega_0$ -resonance mirrors the form of the lowest Bogoliubov band (see Fig. 1). In the other cases, the k -dependence of the growth rates is not that easily characterized. Some insight is gained from the two-mode approximation where, according to expression (33), the k -dependence of the growth rate on resonance is determined by the product

$(\omega_{jk} + \omega_{j'k})\Gamma_{+-}^{jj'}(k)$. Hence, the fact that for the $2\omega_0$ -resonance the growth rate γ has a shape similar to that of ω_{0k} implies that Γ_{+-}^{00} varies little with k . This is confirmed by a direct calculation of Γ_{+-}^{00} through Eq. (19). The result is shown as the solid line in the lower panel of Fig. 7. Conversely, the growth rates of the other resonances in Fig. 3 do not exhibit this behavior, indicating that the corresponding $\Gamma_{+-}^{jj'}$ have a nontrivial dependence on k .

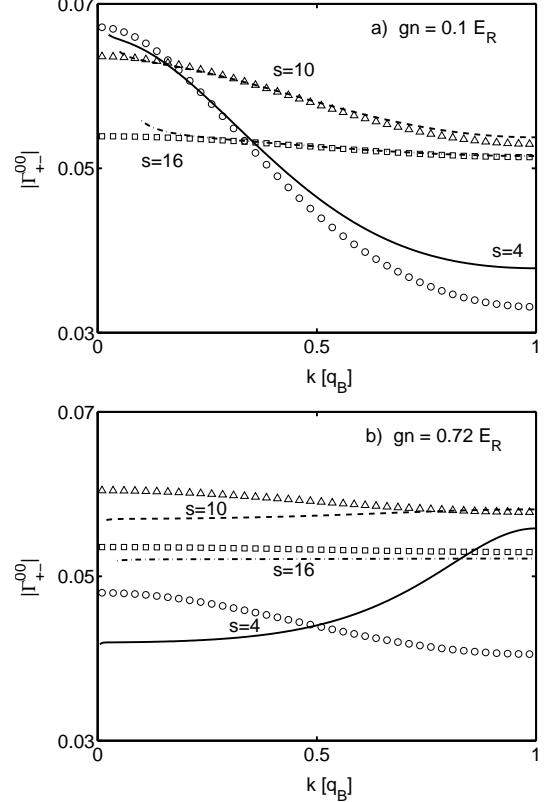


FIG. 7: Coupling Γ_{+-}^{00} between counter-propagating modes of the first Bogoliubov band as a function of quasimomentum k at $gn = 0.1E_R$ (top panel) and $gn = 0.72E_R$ (bottom panel) for different values of the lattice depth $s_0 = 4, 10$ and 16 . Lines: definition (19) with the quasiparticle amplitudes taken from the numerical solution of the Bogoliubov equations (6). Points: Tight binding result (42).

Up to now, our discussion has dealt with the properties of parametric instabilities at a lattice depth which is modulated around $s_0 = 4$. As s_0 is increased, the width of the first Bogoliubov band decreases and, accordingly, the $2\omega_0$ resonance is shifted to lower modulation frequencies Ω . Moreover, an increase of the lattice depth changes the growth rates of parametric amplification. This can be seen in the two-mode approximation where the $2\omega_0$ -growth rate is proportional to s_0 , the Bogoliubov frequency ω_0 and the coupling Γ_{+-}^{00} . In the lower panel of Fig. 7 the quantity Γ_{+-}^{00} is plotted for three different values of s . As one can see, its s dependence is quite weak.

The product $s_0\omega_0$ remains also of the same order, since an increase of s_0 is counterbalanced by a decrease of ω_0 . At zone boundary and for $gn = 0$, their product takes the values 4.2, 5.8, 5.2 E_R for $s_0 = 4, 10, 16$, respectively. This implies that the effects of a variation of s_0 on the timescale of parametric instability of the $2\omega_0$ branch are not dramatic in this range of s_0 . For sufficiently large s_0 one enters the tight binding regime, where ω_0 is proportional to $\sqrt{\delta\kappa^{-1}}$ (see Eq.(39)) and one gets an exponential decrease which eventually dominates the lattice depth dependence of the product $s_0\omega_0$ and hence of the growth rate.

In section IV above, we derived an expression for the coupling Γ_{+-}^{00} in the tight binding regime (see Eqs.(42)-(43)). In Fig. 7 we compare the tight binding results with those obtained from the numerical solution of the Bogoliubov equations (6) for different values of the lattice depth s_0 and two different values of the interaction parameter gn . The numerical results (lines) approach the tight binding results (points) as the lattice is made deeper. For a given s_0 the agreement is better when the interaction parameter gn is lower. For $gn = 0.1E_R$ the agreement is reasonably good already at a lattice depth of $s_0 = 4$, while deeper lattices are necessary to achieve the same degree of agreement for $gn = 0.72E_R$. This is consistent with general arguments on the applicability of the tight binding approximation [18]. A repulsive mean-field interaction causes an effective smoothing of the periodic potential seen by the atoms and therefore the convergence to the tight binding regime is pushed to higher values s_0 .

With reference to Fig. 7 we note that, at fixed s_0 , the coupling Γ_{+-}^{00} takes similar values for the two different interaction parameters gn . However, as pointed out in section II B, the coupling between counter-propagating Bogoliubov modes, which is necessary for parametric amplification, vanishes in the noninteracting case. Numerically we find that the parameter gn has to be tuned to very small values ($\ll 10^{-3}$) before a significant reduction of Γ_{+-}^{00} is achieved.

VI. COMPARISON WITH GP SIMULATIONS

The above discussion of the parametric instability of the condensate is based on a suitable linearization of the 1D GP equation (2). We assumed that most of the atoms are described by an order parameter Ψ_0 , which adiabatically follows the modulations of the lattice depth $s(t)$, plus a small deviation $\delta\Psi$. Under this hypothesis, we have found that $\delta\Psi$ can exhibit an exponential growth as a consequence of the parametric instability of Bogoliubov excitations. The applicability of this approach to actual 3D condensates in experimentally feasible conditions can be tested by comparing its results with those of GP simulations, i.e., a direct numerical integration of the time-dependent GP equation (1).

For condensates subject to strong transverse confine-

ment the integration of the GP equation can be efficiently performed by using the Non-Polynomial Schrödinger Equation (NPSE) introduced in Ref. [28]. The key assumption is that the order parameter can be factorized, as in section II, in the product of a Gaussian radial component and an axial wave function $\Psi(z, t)$. Differently from section II, using the NPSE one assumes the Gaussian to have a z -and t -dependent width, $\sigma(z, t)$. The GP equation (1) thus yields

$$i\hbar\partial_t\Psi = \left[-\frac{\hbar^2}{2m} \left(\partial_z^2 + \frac{1}{\sigma^2} + \frac{\sigma^2}{a_\perp^4} \right) + V + \frac{g_3 N |\Psi|^2}{2\pi\sigma^2} \right] \Psi, \quad (46)$$

and $\sigma = a_\perp(1 + 2aN|\Psi|^2)^{1/4}$. In the geometry of the present work, differences between NPSE and the exact 3D GP equation are negligible and solving the NPSE is much less time consuming. The effective 1D GP equation (2) corresponds to the approximation $\sigma = a_\perp$.

Let us first consider, as in section II, a condensate which is unbound along z , subject to the external potential

$$V(z, t) = \frac{m}{2} \omega_\perp^2 r_\perp^2 + s(t) E_R \sin^2(q_B z), \quad (47)$$

with $s(t)$ given in (11). In order to compare the results with those of the effective 1D GP equation (2) we choose the parameters in (46) and (47) such that the condensate has the same interaction parameter gn , where n is the average linear density.

We first calculate the ground state order parameter Ψ_0 in a static lattice of depth s_0 and then we follow the evolution of Ψ under the modulation $s(t)$, with given A and Ω . The Fourier transform of $\Psi(z, t)$ gives the momentum distribution, $n(k)$, as a function of time. The initial momentum distribution is characterized by the three peaks at $k = 0$ and $k = \pm 2q_B$, associated with the stationary order parameter Ψ_0 in the periodic lattice. As time goes on, we observe a relative oscillation of these peaks with the same frequency of the lattice modulation. This reflects the fact that Ψ_0 adiabatically follows the oscillations of the lattice depth. However, after a certain time a parametric instability becomes visible, that is, the momentum distribution develops components at the momenta $\pm k$ of the amplified Bogoliubov modes. An example is shown in Fig. 8. For even longer times, contributions from momenta throughout the first Brillouin zone start showing up due to higher-order harmonic generation, Bragg reflection and nonlinear coupling between different modes (see [14] for a detailed discussion of the different stages of the evolution).

The degree to which the parametric instability has evolved in time can be quantified by looking at the number of particles δN contributing to the momentum distribution away from the Ψ_0 components. In practice, we calculate the *coherent* part, N_{coh} , by integrating the momentum distribution within the intervals $0 \pm \Delta$ and $\pm 2q_B \pm \Delta$, with $\Delta = q_B/10$, and then we define the incoherent fraction $\delta N/N = (N - N_{\text{coh}})/N$. In Fig. 9,

we plot $\delta N/N$ as a function of time as obtained with a modulation amplitude $A = 0.2$ for two different values of the modulation frequency Ω within the range of the $2\omega_0$ -resonance.

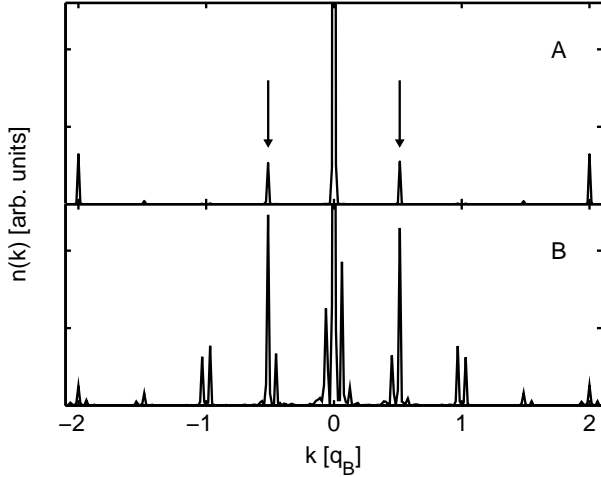


FIG. 8: Momentum distribution of a condensate which is harmonically confined in the radial direction and periodic along z , obtained by performing GP simulations. The interaction parameter is $gn = 0.72E_R$, where n is the average linear density. The optical lattice has $s_0 = 4$ and is modulated with $A = 0.2$ and $\Omega = \omega_R$. The modulation starts at $t = 0$ and the momentum distribution is plotted at $t = t_A$ (top panel) and $t = t_B$ (bottom panel), where A and B are the points indicated in Fig. 9. The arrows show the position of the parametrically unstable modes.

In order to observe the amplification, an initial seed is required. In the calculations a numerical noise is always present and is enough to trigger the instability with long modulation times. Adding an extra noise by hand in the initial order parameter anticipates the time at which the exponential growth becomes visible, but without affecting the growth rate. For the calculations in Figs. 8 and 9 the seed is added in the form of a white numerical noise in $\Psi(z, 0)$. This noise, which is not visible on the scale of Fig. 8, is added in the interval $-q_B < k < q_B$ and corresponds to $\delta N/N$ of the order of 10^{-4} . Only a small part of this noise is subsequently amplified, i.e., the one having the quasimomentum k of the resonant modes. By extrapolating the linear fit to $t = 0$ we see that the seed in Fig. 9 is of the order of 10^{-7} .

We extract the growth rates γ by plotting the data on a logarithmic scale and performing a linear fit in the time interval where the exponential amplification is visible, as indicated by the dashed lines in Fig. 9. The extracted values of γ can be directly compared to the results discussed in the previous sections, which were calculated by an appropriate linearization of the effective 1D GP equation (2). The comparison is shown in Fig. 6. The results of the numerical integration of Eq. (1) are shown as empty squares. The error bars come from the uncertainties in

the fitting procedure on the growth of $\delta N/N$ in the simulations. The overall qualitative agreement is good. The growth rate increases almost linearly with Ω , following the $2\omega_0$ resonance up to the band edge at $k = q_B$. Then it suddenly drops. Weak A^2 -resonances become visible in the gap between the $2\omega_0$ and the $(\omega_0 + \omega_1)$ branches. The agreement is especially good for the lowest $2\omega_0$ resonance. This confirms the accuracy, in this range of Ω , of the approximations made in section II, namely, that the 1D GP equation can be linearized in $\delta\Psi$ via the ansatz (3), with a Ψ_0 which adiabatically follows the modulation of the lattice, and that the inhomogeneous term in (12) is negligible.

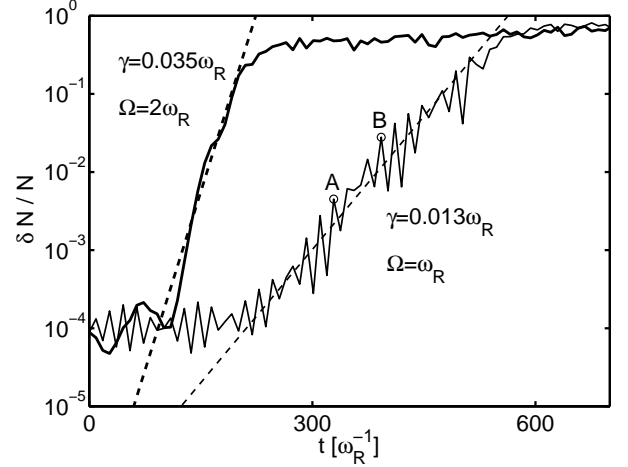


FIG. 9: Incoherent fraction $\delta N/N$ as a function of modulation time obtained by performing time-dependent GP simulations. Solid lines correspond to $s_0 = 4$, $A = 0.2$ and two different modulation frequencies: $\Omega = \omega_R$ and $\Omega = 2\omega_R$. The growth rate γ is extracted from a linear fit (dashed lines). The momentum distribution of the condensate at the instants A and B is shown in Fig. 8.

Now we consider a condensate which is also axially trapped. We solve again Eq. (46), with the external potential

$$V(z, t) = \frac{m}{2}(\omega_\perp^2 r_\perp^2 + \omega_z^2 z^2) + s(t)E_R \sin^2(q_B z). \quad (48)$$

We choose the parameters such as to simulate a single tube of Ref. [15]. So, we use $d = 413$ nm, $\omega_z = 2\pi \times 84.6$ Hz, $\omega_\perp = 2\pi \times 36.5$ KHz and the total number of particles $N = 100$. These values yield $E_R/\hbar = 2\pi \times 3.34$ KHz. These are the same parameters used in our previous work [14]. We extract the growth rate as done above for the simulation with the infinite cylinder. The results for the $2\omega_0$ resonance are shown in Fig. 6 as solid circles. We notice that the number of particles per site in the trapped condensate is z -dependent, so that the comparison with the infinite cylinder of fixed linear density n is subject to some arbitrariness in the definition of the axial average of n in the trap. Nevertheless the agreement is rather satisfactory and supports the physical pictures

discussed in [14] about the key role played by parametric resonances in the experimentally observed response to a lattice modulation in the superfluid regime [15, 16, 17].

Finally, it is worth stressing that GP simulations account for the effects of the nonlinear dynamics associated with the mean-field interaction term in the time dependent GP equation. In particular, when the population of a parametrically unstable mode becomes large, nonlinear processes yield a significant coupling with other nonresonant modes and a consequent redistribution of energy over a wider range of quasimomenta, eventually causing a saturation of the incoherent fraction $\delta N/N$ when it approaches 1, as in the two curves plotted in Fig. 9. Effects of these processes are also visible in part B of Fig. 8. In the case of axially trapped condensates they are enhanced by the finite size of the systems, Z , which introduces a natural broadening of the order $1/Z$ in the momentum distribution (see discussion in [14]). However, an important result of the present analysis is that such nonlinear processes do not prevent the parametric resonances to be observable, either by measuring the final effects of the amplification process (as, for instance, the total energy transferred to the condensate as a function of Ω and A as in [15, 16, 17]) or by looking directly at the exponential growth of the unstable modes in the momentum distribution. In the latter case, the identification of a peak with a rapidly growing height in the measured momentum distribution would also allow one to use the parametric resonances as a spectroscopy tool, namely to measure the dispersion relation ω_{jk} in a parameter space where other spectroscopic techniques, such as two-photon Bragg scattering, are not easily applicable. The timescale and the size of $\delta N/N$ predicted in this work seem well compatible with feasible experiments.

VII. REMARKS ON THERMAL AND QUANTUM SEED

As we already noticed, at the mean-field level the parametric resonances occur only if the relevant Bogoliubov modes are initially occupied. Within the two-mode approximation, discussed in section III, we have shown that a special role is played by the effective seed η defined in (37). This quantity is exponentially amplified in time.

Different mechanisms can cause a non-vanishing η . The condensate can be simply out of equilibrium at the beginning of the modulation due to non-adiabatic processes when it is loaded in the trap and in the optical lattices. This yields some excitations over the ground-state. A similar and controllable seed could be added to the condensate by exciting certain Bogoliubov modes by means of an appropriate external perturbation (e.g., two-photon Bragg scattering) before starting the lattice modulation. Both these types of seed can be described with the GP equation. On the contrary, the GP equation does not account for thermal and quantum fluctuations, which have to be treated with different methods beyond

mean-field.

In sections II and III we treated the collective excitations of the condensate by linearizing the GP equation. We have also used the Bogoliubov quasiparticle amplitudes, solution of Eq. (6), as basis functions to represent the fluctuating component $\delta\Psi$, the coefficients of the expansion (15) being c-numbers related to the population of the collective modes. This allowed us to interpret the dynamics in terms of coupling and growth of Bogoliubov excitations. A natural generalization consists in replacing these c-numbers with the quasiparticle creation and annihilation operators, as in the standard Bogoliubov theory [29]. In such a way one can treat both thermal and quantum fluctuations, under the only assumption that the total number of particles N is macroscopic and the fraction of noncondensed particles is much smaller than N . A direct connection between this quantum treatment of the operator $\delta\Psi$ and our previous approach of section III can be found by using the Wigner representation of the quantum fields [30, 31]. In this way, the dynamics is still governed by the classical equations of sections II and III, but the condensate depletion is now included *via* a stochastic distribution of the coefficients c_{jk} . Exact results can be obtained by averaging over many different realizations of the condensate in the same equilibrium conditions. In particular, one has

$$\langle c_{jk}(0) \rangle = 0 \quad , \quad \langle c_{jk}(0) c_{j'k}(0) \rangle = 0 , \quad (49)$$

$$\langle c_{jk}(0) c_{j'k'}^*(0) \rangle = \left[\frac{1}{2} + \frac{1}{e^{\beta\hbar\omega_{jk}} - 1} \right] \delta_{jj'} \delta_{kk'} , \quad (50)$$

where $\beta = (k_B T)^{-1}$. The $1/2$ term in (50) describes quantum fluctuations and is the leading one at small T , while the second term accounts for thermal fluctuations. One can make use of (49)-(50) to evaluate the mean effective seed defined in (37), finding

$$\langle |\eta|^2 \rangle = \frac{1}{4} \left(1 + \frac{1}{e^{\beta\hbar\omega_{jk}} - 1} + \frac{1}{e^{\beta\hbar\omega_{j'k}} - 1} \right) . \quad (51)$$

Equation (51) provides a way to extract information about the initial seed from the measurement of the exponential growth of the incoherent fraction. For example, within the two mode approximation described in section III, one finds that the number of particles in the modes j and j' at $t \gg \gamma_{\max}^{-1}$, averaged over many realizations, grows as

$$\langle \delta N \rangle = C \langle |\eta|^2 \rangle e^{2\gamma_{\max} t} , \quad (52)$$

with $C = \int_{-d/2}^{d/2} dz (|\tilde{u}_{jk}|^2 + |\tilde{v}_{jk}|^2 + |\tilde{u}_{j'k}|^2 + |\tilde{v}_{j'k}|^2)$. So, if one is able to measure $\langle \delta N \rangle$ at different times during the parametric amplification and extract its value at $t = 0$ from a fit, then Eqs. (51) and (52) give direct information on the quantum or thermal nature of the seed, provided the Bogoliubov spectrum of the condensate is known.

The thermal regime is obtained when $k_B T \gg \hbar\omega_{jk}$ and corresponds to the “classical” limit where the occupation numbers of the relevant modes are large. In

this regime, the parametric response of the system to the lattice modulation can provide a thermometry. Let us suppose, in fact, that an experiment is set up to observe the exponential growth at $\Omega = 2\omega_{0k}$, as in the simulation of Fig. 9, and that the dispersion law ω_{0k} is also known (either from calculations or by direct measurements of $n(k)$). Equation (51) predicts $\langle|\eta|^2\rangle \simeq (1/2)k_B T/\hbar\omega_{0k}$ for $k_B T \gg \hbar\omega_{0k}$, so that the knowledge of the spectrum and the average seed vs. k provides an estimate of the temperature T . If the fit works well this means that the gas of excitations is in thermal equilibrium. This is an important result in view of the fact that the temperature we are speaking about can be much smaller than the temperatures which can be measured with current techniques, based on the detection of the thermal cloud. In the absence of a visible thermal cloud, parametric resonances appear to be an interesting method to make small thermal fluctuation detectable *via* a selective amplification.

The other important limiting case is that encountered when $k_B T \ll \hbar\omega_{jk}$. In this condition the initial population of the unstable modes is mainly due to quantum fluctuations and $\langle|\eta|^2\rangle \sim 1/4$. The modulation of the lattice thus acts on the quantum vacuum, squeezing it and transferring energy to the system. So, even at $T = 0$, one can parametrically excite the condensate by amplification of the vacuum fluctuations and this is a signature of its underlying quantum nature. This regime is analogous to the parametric down conversion, a well-known phenomenon in nonlinear quantum optics [31]. A conceptually interesting point is that the amplification of quantum fluctuations acts as a source of entangled quasiparticles, analogous to parametric sources of entangled photon pairs in quantum optics [32]. A particularly appealing case is that of a modulation frequency Ω such as to resonantly excite two counter-propagating quasiparticles in different bands, j and j' . In this case, the quasiparticle pair is represented by the entangled state

$$|\Psi\rangle \propto |j, k\rangle|j', -k\rangle + |j, -k\rangle|j', k\rangle. \quad (53)$$

A quite similar situation has been recently discussed for the generation of branch-entangled polariton pairs in microcavities through spontaneous interbranch parametric scattering [33]. It is finally worth mentioning that the creation of quasiparticle pairs out of vacuum fluctuations can also be viewed as a manifestation of a dynamic Casimir effect: the environment in which quasiparticles live is periodically modulated in time and this modulation transforms virtual quasiparticles into real quasiparticles [34].

VIII. CONCLUSIONS AND OUTLOOK

In this work we have explored the origin and the effects of parametric resonances in elongated Bose-Einstein condensates subject to a 1D optical lattice whose intensity is periodically modulated in time. We have used a suitable linearization of the time-dependent GP equation to calculate the stability diagram and the growth rate of unstable modes. We have shown that the main mechanism of instability is a coupling between pairs of counter-propagating Bogoliubov excitations. This coupling is caused by the modulation of the background in which the excitations live. This picture emerges quite clearly when a two-mode approximation is considered. In this case, one can derive semi-analytic results for the coupling between Bogoliubov modes in different bands and discuss the convergence to the tight binding regime. The results have been compared with those of time-dependent GP simulations, for both condensates which are infinite and trapped in the axial direction. The overall agreement supports the interpretation of our previous GP simulations [14], which were aimed at explaining the response to the lattice modulation observed in the experiments of Refs. [15, 16, 17] in the superfluid regime. Our analysis also suggests the possibility to perform new experiments in order to observe the effects of the parametric resonances in a more controllable way as a tool for a novel type of spectroscopy and, possibly, for a characterization of quantum and/or classical seeds in actual condensates. Along this line, our final discussion about the role of the seed and the applicability of the Wigner representation is more intended to be a suggestion for future work rather than a quantitative analysis. This topic certainly deserves further investigations.

Our formalism can be naturally generalized to different types of periodic modulations and different geometries. An interesting example is the periodic translation (shaking) of the optical lattice as in the recent experiment of Ref. [35]. Another simple case is the modulation of the transverse trapping frequency in elongated condensates with or without optical lattice. Work in this direction is in progress [36].

Acknowledgments

We are particularly indebted to I. Carusotto for valuable suggestions and comments. Fruitful discussions with M. Modugno and L. Pitaevskii are also acknowledged. One of us (M.K.) thanks the DFG for support.

[1] L.D. Landau and E.M. Lifshitz, *Mechanics* (Oxford, Pergamon, 1973).
[2] V.I. Arnold, *Mathematical Methods of Classical Mechanics* (Springer-Verlag, Berlin, 1989).
[3] Y. Castin and R. Dum, Phys. Rev. Lett. **79**, 3553 (1997).
[4] Yu. Kagan and L.A. Maksimov, Phys. Rev. A **64**, 53610 (2001).
[5] P.G. Kevrekidis, A.R. Bishop, and K.O. Rasmussen, J.

Low Temp. Phys. **120**, 205 (2000)

[6] J.J. García-Ripoll, V.M. Pérez-García, and P. Torres, Phys. Rev. Lett. **83**, 1715 (1999).

[7] K. Staliunas, S. Longhi, and G.J. de Valcárcel, Phys. Rev. Lett. **89**, 210406 (2002).

[8] L. Salasnich, A. Parola, and L. Reatto, J. Phys. B: At. Mol. Opt. Phys. **35**, 3205 (2002)

[9] G.L. Salmond, C.A. Holmes, and G.J. Milburn, Phys. Rev. A **65**, 033623 (2002).

[10] H.L. Haroutyunyan and G. Nienhuis, Phys. Rev. A **70**, 063603 (2004).

[11] Z. Rapti, P.G. Kevrekidis, A. Smerzi, and A.R. Bishop, J. Phys. B: At. Mol. Opt. Phys. **37**, S257 (2004).

[12] F. Dalfovo, S. Giorgini, L.P. Pitaevskii and S. Stringari, Rev. Mod. Phys. **71**, 463 (1999).

[13] L. Pitaevskii and S. Stringari, *Bose-Einstein condensation* (Clarendon Press, Oxford, 2003).

[14] M. Krämer, C. Tozzo, and F. Dalfovo, e-print cond-mat/0410122, Phys. Rev. A, in press.

[15] T. Stöferle, H. Moritz, C. Schori, M. Köhl, and T. Esslinger, Phys. Rev. Lett. **92**, 130403 (2004).

[16] M. Köhl, H. Moritz, T. Stöferle, C. Schori, and T. Esslinger, J. Low Temp. Phys. **138**, 635 (2005).

[17] C. Schori, T. Stöferle, H. Moritz, M. Köhl, and T. Esslinger, Phys. Rev. Lett. **93**, 240402 (2004).

[18] M. Krämer, C. Menotti, L. Pitaevskii, S. Stringari, Eur. Phys. J. D **27**, 247 (2003).

[19] K. Berg-Sørensen, K. Mølmer, Phys. Rev. A **58**, 1480 (1998).

[20] M.L. Chiofalo, M. Polini, M.P. Tosi, Eur. Phys. J. D **11**, 371 (2000).

[21] S.A. Morgan, S. Choi, K. Burnett, and M. Edwards, Phys. Rev. A **57**, 3818 (1998); P.B. Blakie, R.J. Ballagh, and C.W. Gardiner, Phys. Rev. A **65**, 033602 (2002).

[22] C. Tozzo and F. Dalfovo, Phys. Rev. A **69**, 053606 (2004).

[23] One can prove that $\partial_t \sum_j |c_{jk}|^2 = 0$, when $\Gamma_{+-}^{jj'} = 0$, by using Eq. (16) and noticing that $\Gamma_{++}^{jj'} + (\Gamma_{++}^{jj'})^* = 0$ due to the ortho-normalization conditions (9).

[24] R.B. Shirts, ACM Transactions on Mathematical Software **19**, 377 (1993).

[25] W. Magnus and S. Winkler, *Hill's Equation* (Dover, New York, 1979).

[26] The analogous case in quantum optics is treated in Ref. [31], chapter 5.1.

[27] Note that, if the modulation (11) is changed by a phase $\Delta\phi$, the results (37)-(38) will still apply, but with $\phi = \text{phase}(\bar{\gamma}) + \Delta\phi$, which means that a different quadrature is amplified.

[28] L. Salasnich, A. Parola, and L. Reatto, Phys. Rev. A **65**, 043614 (2002).

[29] N.N. Bogoliubov, J. Phys. (Moscow) **11**, 23 (1947).

[30] A. Sinatra, Y. Castin, C. Lobo, J. Mod. Opt. **47**, 2629 (2000).

[31] D.F. Walls and G.J. Milburn, *Quantum Optics*, (Springer Verlag, Berlin, 1994).

[32] Pa.G. Kwiat, K. Mattle, H. Weinfurter, A. Zeilinger, A.V. Sergienko and Y. Shih, Phys. Rev. Lett. **75**, 4337 (1995).

[33] C. Ciuti, Phys. Rev. B **69**, 245304 (2004).

[34] The analogous case of photons created in an oscillating cavity is treated, for instance, in A. Lambrecht, M.-T. Jaekel, and S. Reynaud, Phys. Rev. Lett. **77**, 615 (1996). See also C. Braggio *et al.*, quant-ph/0411085 and references therein.

[35] N. Gemelke, E. Sarajlic, Y. Bidel, S. Hong, and S. Chu, e-print cond-mat/0504311. The purpose of this work was the observation of a period-doubling instability analogous to similar dynamical instabilities in a condensate moving in an optical lattice. In addition to the period-doubling instability, an unexpected type of excitations was observed at higher modulation frequency. We guess that this could be the result of the parametric resonance at the frequency $\omega_0 + \omega_1$, which is the lowest one allowed by the symmetry of the problem.

[36] M. Modugno, C. Tozzo, and F. Dalfovo, in preparation.